Empirical wavelet transform and dual feed-forward neural network for classification of power quality disturbances

Karthik Thirumala*

Department of Electrical and Electronics Engineering,
National Institute of Technology Tiruchirappalli, India
Email: karthikt2707@gmail.com
*Corresponding author

Aditi Kanjolia, Trapti Jain and
Amod C. Umarikar

Department of Electrical Engineering,
Indian Institute of Technology Indore,
Indore, 453552, India
Email: aditi7kanjolia@gmail.com
Email: traptij@iiti.ac.in
Email: umarikar@iiti.ac.in

Abstract: This paper proposes a novel approach for classification of single and combined power quality (PQ) disturbances. The EWT-based adaptive filtering technique is employed first to decompose the signal into its individual frequency components by estimation of frequencies. The frequency estimation in this paper is done using a divide-to-conquer principle-based FFT technique and followed by an adaptive filter design. Then, some unique potential features reflecting the characteristics of disturbances are extracted from the mono-frequency components as well as the signal. A single classifier used for the classification of combined disturbances, whose characteristics are alike, gives less classification accuracy. Therefore, the use of a dual FFNN is proposed for the classification of single and combined PQ disturbances to effectively reduce the misclassification and improve the accuracy. The effectiveness of the proposed approach is evaluated on a broad range of time-varying power signals with varying degree of irregularities, noise, and fundamental frequency deviation. The results obtained for both the simulated as well as the real disturbance signals elucidate the efficiency and robustness of the proposed approach for classification of the most frequent disturbances.

Keywords: power quality; PQ; fast Fourier transform; FFT; empirical wavelet transform; EWT; adaptive filtering; dual feed-forward neural network.

Reference to this paper should be made as follows: Thirumala, K., Kanjolia, A., Jain, T. and Umarikar, A.C. (2020) 'Empirical wavelet transform and dual feed-forward neural network for classification of power quality disturbances', *Int. J. Power and Energy Conversion*, Vol. 11, No. 1, pp.1–21.

Biographical notes: Karthik Thirumala is currently working as an Assistant Professor in the Department of Electrical and Electronics Engineering, National Institute of Technology, Tiruchirappalli, India. His research interest includes power quality analysis and power electronics applications to power systems.

Aditi Kanjolia received her BTech in Electrical Engineering from the Indian Institute of Technology Indore, Indore, India in 2016. Her research interests include power quality analysis and artificial intelligence.

Trapti Jain is an Associate Professor in the Department of Electrical Engineering, Indian Institute of Technology Indore, Indore, India. Her research interests include power systems security, artificial-intelligence applications to power systems, power system dynamics and power quality.

Amod C. Umarikar is an Associate Professor in the Department of Electrical Engineering, Indian Institute of Technology Indore, Indore, India. His research interests include the application of power electronics in renewable energy systems and power quality.

1 Introduction

The extreme usage of nonlinear and electronic controlled loads, smart transmission systems, and variations in load exaggerate various power quality (PQ) issues. Besides, the consistent increase in penetration of renewable energy-based distributed generation (DG) worsens these problems further. The PQ problems manifested cover a broad range of amplitude variation along with the existence of new frequencies causing disturbances such as voltage sag/swell, voltage imbalance, voltage fluctuation and harmonics/interharmonics distortion (Dugan et al., 2012). The economic operation of the system while maintaining good PQ has become one of the prime objectives in the development of smart grid. In order to improve the quality of power supply by using an appropriate mitigation device, it is essential to identify the frequently occurring PQ disturbances and their sources (IEEE, 2009). Therefore, it has become a practice for the system operators (Milanovic et al., 2014) to continuously monitor and classify these disturbances. Since the characteristics of each PQ disturbance is unique, their recognition can be achieved by extraction of some potential features of the signal using a signal processing approach and then employ a soft computing/intelligent technique for classification (Lieberman et al., 2011; Saini and Kapoor, 2012). In general, based on the characteristics, the PQ disturbances are categorised into stationary disturbances like sag, interruption, swell, harmonics, and non-stationary disturbances such as transient and flicker. The recognition of all single PQ disturbances can be achieved easily by successful utilisation of some standard features together with a simple classifier (He et al., 2013; Zhang et al., 2011; Deokar and Waghmare, 2014). However, it is worth mentioning that in the recent years, the simultaneous occurrence of PQ disturbances is elevated significantly, necessitating the development of new automatic detection algorithms for classification of single and combined PQ disturbances (Andrade et al., 2016; Ferreira et al., 2015; Rodriguez et al., 2014; Kanirajan and Kumar, 2015).

Several methods have been proposed and successfully utilised for pre-processing the power signals such as fast Fourier transform (FFT), discrete wavelet transform, empirical

mode decomposition (EMD), Hilbert-Huang transform (HHT), S-transform (ST), variational mode decomposition (VMD), etc. (Deokar and Waghmare, 2014; Andrade et al., 2016; Kanirajan and Kumar, 2015; Mishra et al., 2008; Abdoos et al., 2016; Hu et al., 2008). The performance of wavelet transform-based segmentation is dependent on the proper selection of mother wavelet and decomposition levels. Also, features extracted from the detail coefficients are more sensitive to the noise present in the signal. The HHT, which includes EMD and Hilbert transform (HT) for extracting the instantaneous information, has the main limitation of mode mixing, which affects the features and degrades the classification performance. Another most commonly employed time-frequency technique; ST utilises a frequency dependent Gaussian window for better capturing of time localised variations, but with high computational complexity (Biswal and Dash, 2013). Furthermore, implementation of these aforementioned algorithms has the limitation of capacity and capability problems (Krishna and Baskaran, 2013). Considering the practical advantages of the FFT, efforts are being made for the development of new techniques based on the FFT (Gallo et al., 2004; Zeng et al., 2013) to enhance its performance. One such technique is the empirical wavelet transform (EWT), (Gilles, 2013; Gilles et al., 2014) which gained a greater attention for analysis of non-stationary signals in various applications because of its adaptiveness, simplicity, and fastness. The frequency estimation procedure of the EWT was modified in Thirumala et al. (2015) to make it suitable for PQ analysis by estimating only significant frequencies from the spectrum using a minimum magnitude (*dM*) and minimum frequency distance threshold (*dF*). The thresholds were conceived to estimate the harmonics and interharmonics present in the signal, and thereby the PQ indices accurately. However, to characterise a short duration PQ disturbance, it is always preferred to consider the window length of 200 ms with a frequency resolution of 5 Hz in accordance to the IEC standard 61000-4-7 (IEC, 2002). The consequent decrease in frequency resolution and an increase in spectral leakage due to the non-stationary nature may result in imperfect decomposition of the input signal. This can be overcome by estimating the harmonics and interharmonics separately based on the divide to conquer principle.

The feature selection is one of the extremely important tasks for the classification problems. The next stage involves extraction of some significant features that hold the characteristics of PQ disturbances. Few such features are the root mean square (RMS) values, total harmonic distortion (THD), energy, mean, variance and standard deviation (Biswal and Dash, 2013; Manikandan et al., 2015; Lee and Shen, 2011). The performance of a classification problem depends not only on the signal decomposition and features employed but also on the ability of the classifier. These extracted features are subsequently used by the classifiers based on decision tree (DT), fuzzy logic, K-nearest neighbour (KNN), support vector machines (SVM) and artificial neural network (ANN) for classification of PQ disturbances (Zhang et al., 2011; Deokar and Waghmare, 2014; Rodriguez et al., 2014; Kanirajan and Kumar, 2015; Mishra et al., 2008; Abdoos et al., 2016; Hu et al., 2008; Manikandan et al., 2015; Lee and Shen, 2011; Panigrahi and Pandi, 2009; Liu et al., 2015; Santoso et al., 2000). It has been observed from the literature that the DT classifiers are flexible to handle, but can detect only single disturbances accurately with thresholds according to the IEEE std. 1159 (IEEE, 2009) and IEC 61000-4-7 (IEC, 2002). The expert systems fall under deterministic method and are normally slow in execution. The fuzzy classifiers lack self-learning capability and need an expert for rulemaking because of which they are not appropriate for PQ disturbances

classification. In the recent years, the support vector machine, which is a statistical approach, has gained greater interest due to the leading advantages of structural and empirical risk minimisation principle. However, the main problem with the SVM involves solving the complex quadratic optimisation problem for larger datasets. As the number of classes' increases, the complexity also increases, and the possibility of misclassification is obvious. Henceforth, the multi-class SVMs are utilised to detect at most fourteen PQ disturbances successfully. Although these approaches are very useful in the classification, only a few of them can effectively detect the real disturbances. ANNs provide an attractive solution to the above classification problem because of their self-learning, cognitive and mathematical flexibility features. If the PQ events are more and the data is abundant, the ANNs are preferred over expert system and SVM. Also, the ANNs are recommendable for real-time applications, which is of interest to the electric power community due to their low time consumption. Therefore, most of the classification systems developed for classification of PQ disturbances is based on ANN. Despite an extensive work carried out in the area of classification of PQ disturbances, there is still a need for the development of new adaptive techniques that can precisely detect the combined disturbances. In the practical scenario where different disturbances coexist resulting in mixed characteristics; employing a single classifier for recognition of all the combined disturbances would reduce the recognition ability of the classifier. At the same time, utilising multiple classifiers (Santoso et al., 2000) to increase the recognition accuracy may also increase the computational time (training and testing). Keeping in view of the fact that ANNs have an added advantage of excellent parallel processing capability unlike other techniques, the use of multiple ANNs can attain improved accuracy with not much increase in computational time. Henceforth, this paper proposes the utilisation of two feed-forward neural networks (FFNNs), each dedicated to recognising four single disturbances.

Thus, this work aims at extraction of some useful features from the EWT-based adaptive filtering technique and then employing a dual FFNN for accurate classification of the most significant combined disturbances with less computational time. The features extracted from the adaptive filtering are informative, unique, easy to extract and also robust to noise. The proposed approach, developed on the basis of an idea presented in (Gallo et al., 2004; Rodriguez et al., 2014) can be summarised in four stages:

1 divide to conquer principle-based frequency estimation

2 signal decomposition using adaptive filters

3 feature extraction from the mono-frequency components

4 finally, building a dual FFNN for the classification of disturbances.

The FFT-based frequency estimation is performed twice, first to estimate fundamental frequency and harmonics, and then to estimate the interharmonics. Then filters are designed according to the frequency information to extract the mono-frequency components as explained in Section 2. Thereby, the proposed method first segments the input signals using the adaptive filtering technique and then extracts some unique features listed in Section 3.1. Thereafter, the extracted features are fed as inputs to the dual FFNN for classification of 18 PQ disturbances (eight single and ten combined) as explained in Section 3.2. Section 4 presents the experiments carried out and the results obtained for both synthetic as well as real disturbance signals. The novelty of the proposed approach

includes detection of disturbance half cycle for feature extraction, feature *F*7 (explained in Section 3.1) and finally, the dual ANNs to attain higher recognition accuracy. Another major contribution of this work is the use of a divide to conquer principle-based frequency estimation procedure for decomposition of disturbance signals.

2 Methodology

2.1 Empirical wavelet transform

This section presents a brief review of EWT, proposed by Gilles (2013). The approach first segments the Fourier spectrum and then builds the empirical wavelet filters accordingly to extract the different modes of the discrete signal $x(k)$. The computational steps of the EWT can be outlined as follows.

1 The FFT of the windowed signal is first calculated to estimate the dominant frequencies present in the signal $f = \{f_i\}_{i = 1, 2, \ldots, N}$.

2 Then segment the spectrum by identifying the boundaries $\Omega = \{\Omega_i\}_{i = 0, 1, \ldots, N}$ that separate two successive frequency components. The first boundary Ω_0 is assumed zero, and the rest $\Omega_i \; \forall i \in [1, N-1]$ are obtained from the local minima between two frequencies f_i, f_{i+1} (Gilles et al., 2014) as shown in Figure 1(a).

3 Based on the frequencies and boundaries estimated, build N empirical wavelet filters in the frequency domain as shown in Figure 1(b) using the below equations.

$$\phi_1(\omega) = \begin{cases} 1 & \text{if } |\omega| \le (1-\gamma)\Omega_1 \\ \cos\left(\frac{\pi}{2}\beta(\gamma, \omega, \Omega_1)\right) & \text{if } (1-\gamma)\Omega_1 \le |\omega| \le (1+\gamma)\Omega_1 \\ 0 & \text{otherwise} \end{cases} \tag{1}$$

$$\psi_i(\omega) = \begin{cases} 1 & \text{if } (1+\gamma)\Omega_i \le |\omega| \le (1-\gamma)\Omega_{i+1} \\ \cos\left(\frac{\pi}{2}\beta(\gamma, \omega, \Omega_{i+1})\right) & \text{if } (1-\gamma)\Omega_{i+1} \le |\omega| \le (1+\gamma)\Omega_{i+1} \\ \sin\left(\frac{\pi}{2}\beta(\gamma, \omega, \Omega_i)\right) & \text{if } (1-\gamma)\Omega_i \le |\omega| \le (1+\gamma)\Omega_i \\ 0 & \text{otherwise} \end{cases} \tag{2}$$

where $\beta(\gamma, \omega, \Omega_i) = \beta(1 / 2\gamma\Omega_i(|\omega| - (1-\gamma)\Omega_i))$ is an arbitrary function fulfilling the properties given in Gilles (2013). The parameter γ ensures very minimal overlap of the two following transition areas, whose selection is based on the boundaries estimated.

4 The approximation and detail coefficients are obtained from the inverse Fourier transform of the filtered spectrum.

$$W_x(1, n) = IFFT(X(\omega)\phi_1(\omega)) \tag{3}$$

$$W_x(i, n) = IFFT(X(\omega)\psi_i(\omega)) \tag{4}$$

The adaptiveness of scaling and empirical wavelet filters makes this technique applicable for analysis of non-stationary signals. However, segmentation of the Fourier spectrum is the most important step, which provides complete adaptiveness and accuracy. Therefore, the frequency estimation stage is modified to make it suitable for analysis of all PQ disturbances.

Figure 1 (a) Segmented Fourier spectrum (b) Spectrum with its corresponding wavelet filters (see online version for colours)

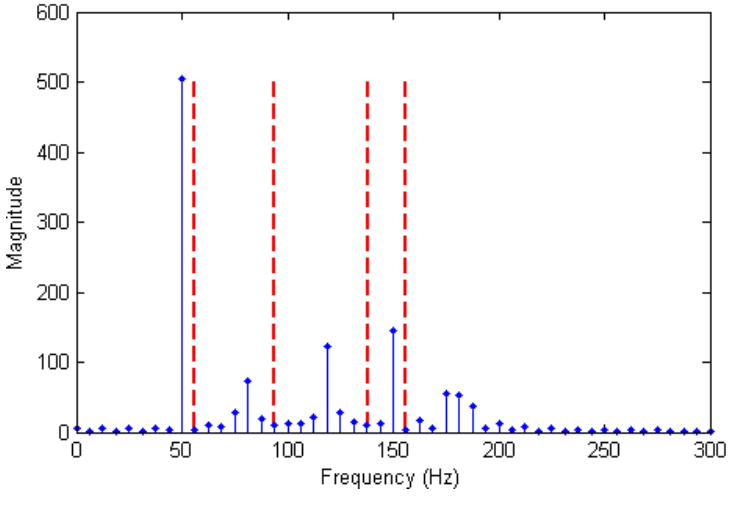

(a)

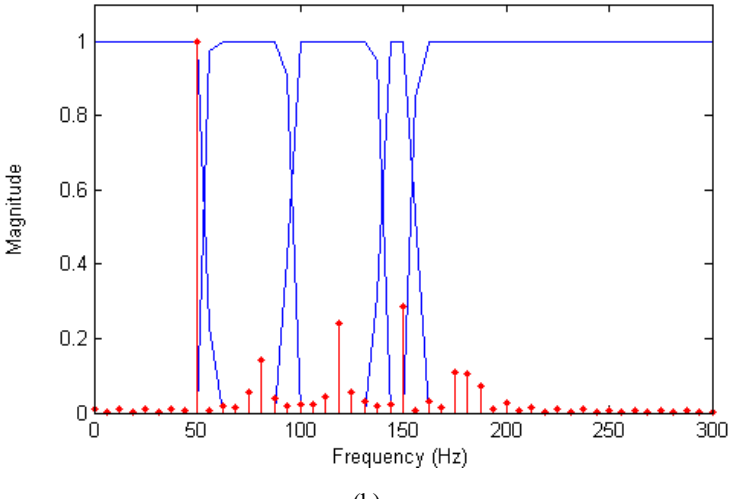

(b)

Figure 2 Adaptive filtering technique for decomposition of an input signal

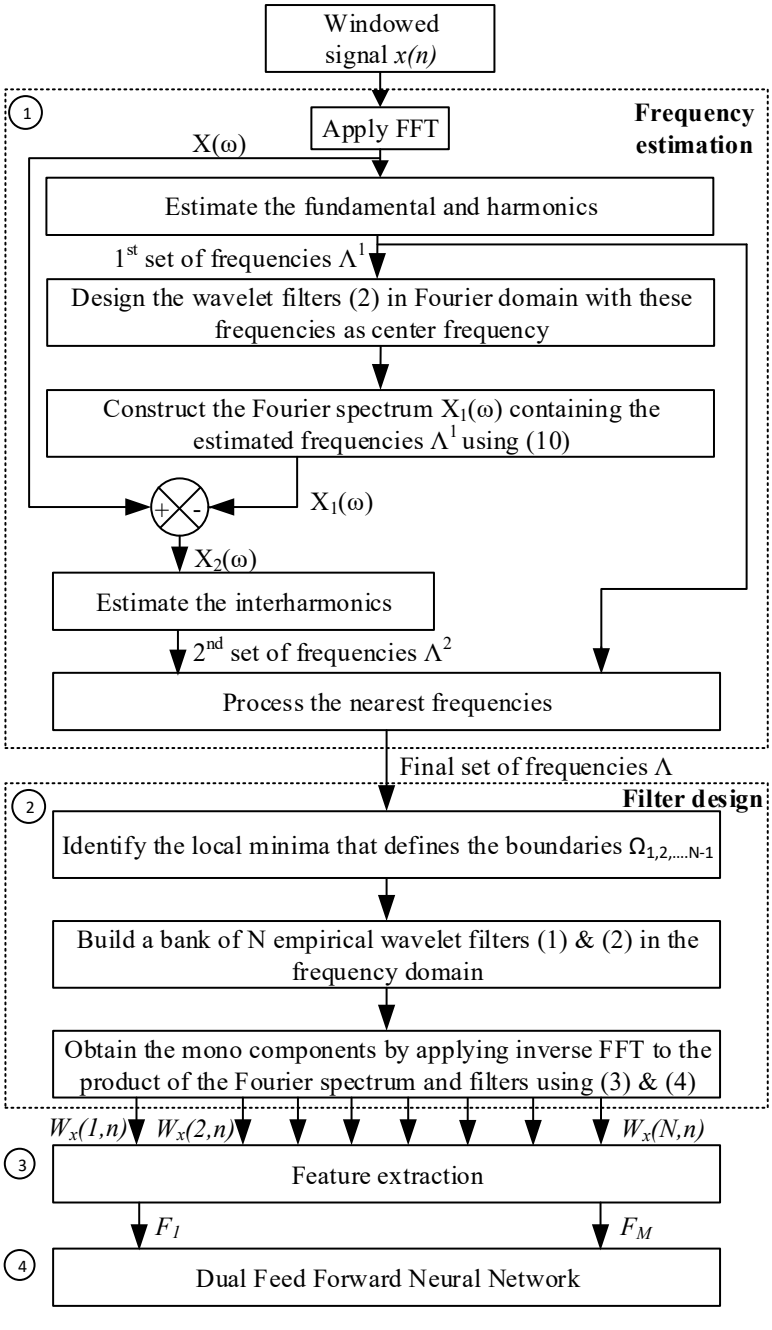

2.2 Adaptive filtering technique

The EWT-based adaptive filtering approach, shown in Figure 2, aims a perfect decomposition of the disturbance signal yielding some robust features for classification of disturbances. The Fourier spectrum of the signal containing harmonics and interharmonics looks complicated, but it can be inferred that the distance between two successive harmonics or two successive interharmonics is relatively more when compared to the distance between an interharmonic and harmonic. Considering this, a divide to conquer principle-based frequency estimation is opted for estimation of harmonics and interharmonics. First, only dominant frequencies $\Lambda^1 = \{f_i\}_{i = 1, 2, \ldots M1}$ containing fundamental frequency and harmonics are estimated using $dM = 2\%$ of the fundamental magnitude and $dF = 45$ Hz. Considering these set of frequencies as centre frequencies, design the empirical wavelets $\psi_i(\omega)$ given in (2) with $\Omega_i = f_i - 5$, $\Omega_{i+1} = f_i + 5$ Hz and $\gamma = 0.01$. The bandwidth of these bandpass filters can be provided by $BW_i = 10 + 2\gamma f_i$ Hz. Then the harmonic spectrum $X_1(\omega)$ can be obtained using

$$X_1(\omega) = \left(\sum_{i \in \Lambda^1} X(\omega)\psi_i(\omega) \right) \tag{5}$$

The subtraction of harmonic spectrum $X_1(\omega)$ from the original spectrum $X(\omega)$ results in a residual spectrum $X_2(\omega)$, which contains only interharmonics. Now estimate the interharmonics $\Lambda^2 = \{f_i\}_{i=1, 2, \ldots, M2}$ by setting $dM = 2\%$ of the fundamental and $dF = 5$ Hz. Concatenate the two set of frequencies and arrange in ascending order to obtain the complete set of frequencies $\Lambda^3 = \{f_i\}_{i = 1, 2, M1 + M2}$. For an extreme non-stationary signal, the information related to the fundamental component and dominant harmonics will still remain in the residual spectrum $X_2(\omega)$ due to spectral leakage. Therefore, in the cumulative set Λ^3, a grouping of directly adjacent components (±5 Hz) is performed to ensure that only the actual frequencies are considered for filter design resulting in specific mono-frequency components. Thus, the post-processing frequencies $\Lambda = \{f_i\}_{i = 1, 2, \ldots, N}$, where $N \leq M1 + M2$, are the final set of frequencies that actually exist in the signal. Therefore, all the frequency components, which are at least 10 Hz apart can be estimated and decomposed by obtaining the boundaries as explained earlier. Then design the empirical wavelet filters according to the frequency information. The components decomposed are of mono-frequency and thereby the extracted features are significant for characterisation of disturbances.

3 Feature extraction and classifier

The block diagram, shown in Figure 3 illustrates the data flow of the proposed approach for classification of PQ disturbances. Since it is extremely difficult to directly utilise the signal for classification of disturbances due to its large data length, an extraction of a minimal set of features will ease the characterisation of disturbances. The features extracted in this paper are non-complex and are computed from the signal information, root-mean-square values of the fundamental component and high-frequency harmonic distortion. Further, the computation of features from the half cycle, which has disturbance is much preferable than extracting features from the whole signal. Thus, the primary step

to be performed before feature extraction is the identification of a half cycle of the input signal where the waveform deviation initiates.

First, compute the RMS for each fundamental half cycle of the input signal as defined

$$X_{rms}(n) = \frac{1}{\sqrt{2}} \sqrt{\frac{1}{S} \sum_{i=(n-1)S+1}^{nS} x(i)^2} \tag{6}$$

where $X_{rms}(n)$ is n^{th} half cycle RMS of the discrete signal $x(i)$ and S is the number of samples in a half cycle. The windowed signal of 200 ms duration having 50 Hz as the fundamental frequency will give a signal RMS vector X_{rms} having values calculated for 20 half cycles as

$$X_{rms} = \left[X_{rms}(1), \ldots, X_{rms}(n), \ldots, X_{rms}(20) \right] \tag{7}$$

Figure 3 Proposed approach for classification of disturbances

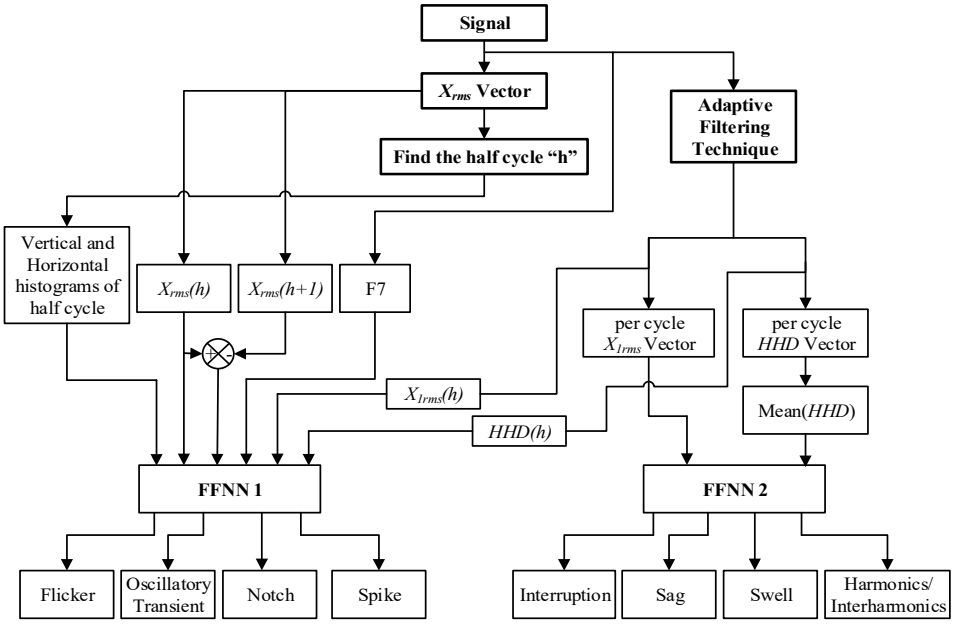

The deviation of two consecutive half cycles exceeding a predefined value of 0.01 indicates the presence of disturbances.

$$\left| X_{rms}(n) - X_{rms}(n-1) \right| \geq 0.01 \quad \forall n = 2, \ldots, 20 \tag{8}$$

The condition given in (8) is satisfied for disturbances such as voltage interruption, sag, swell, flicker, and transient. Thereby, the disturbance half cycle, h is the n^{th} half cycle satisfying the given condition. For the voltage sag signal, shown in Figure 4(a), RMS is calculated for twenty half cycles and the disturbance half cycle, h is found to be seven. The condition fails for steady state disturbances like notch, spike and harmonics, and hence, h is taken as the first half cycle.

Figure 4 (a) Voltage sag signal (b) Detected half cycle (c) Horizontal histogram (d) Vertical histogram (see online version for colours)

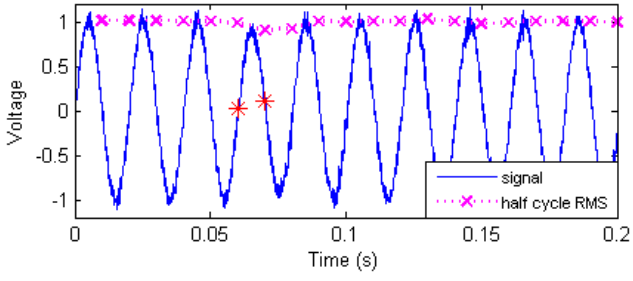

(a)

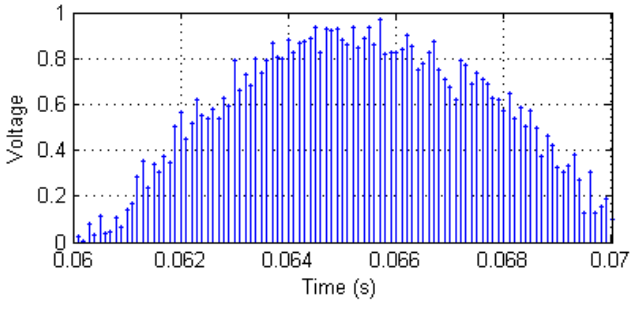

(b)

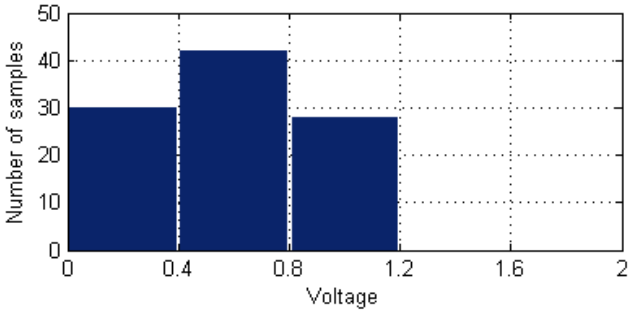

(c)

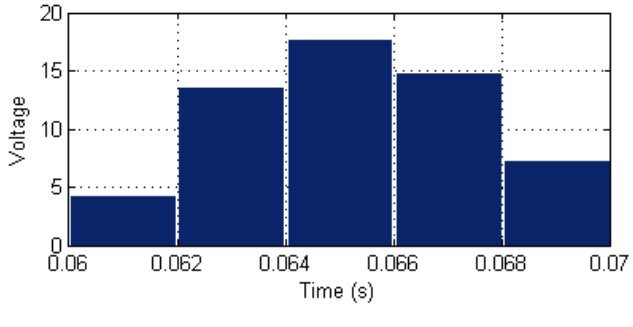

(d)

3.1 Feature extraction

After successful detection of the disturbance half cycle (h), shown in Figure 4(b) (stem plot), the vertical and horizontal histograms (Rodriguez et al., 2014) of that half cycle are obtained to know the nature of the waveform.

F1 The horizontal histogram gives information of the number of times the values appear in a range of 0.4. Thereby, the magnitude from 0 to 2 pu in a range of 0.4 will give five values of the horizontal histogram as shown in Figure 4(c).

F2 The vertical histogram shown in Figure 4(d), is the sum of the signal magnitudes in a range of 2 ms. Hence, five values of vertical histograms are calculated for a half cycle of 10 ms duration.

F3 The RMS value of the disturbance half cycle of the input signal is considered as the third feature.

$$F3 = X_{rms}(h) \tag{9}$$

F4 This feature represents the amount of deviation of the disturbance half cycle (h) with its consecutive half cycle (Zhang et al., 2011), computed as

$$F4 = \left| X_{rms}(h) - X_{rms}(h+1) \right| \tag{10}$$

F5 The RMS value of the fundamental frequency component extracted from the adaptive filtering technique plays a key role in the discrimination of flicker, notch, and spike from the fundamental magnitude related disturbances. Thus, the feature *F5* is the RMS value of the fundamental component calculated for only h half cycle.

$$F5 = X_{1rms}(h) = \frac{1}{\sqrt{2}} \sqrt{\frac{1}{S} \sum_{i=(h-1)S+1}^{hS} x_1(i)^2} \tag{11}$$

F6 The high-frequency harmonic distortion $HHD(h)$ separates all the harmonics related signals from other class of signals (Thirumala et al., 2016).

$$HHD(h) = \frac{X_{Hrms}(h)}{X_{1rms}(h)} \tag{12}$$

where $X_{1rms}(h)$ represents the h half cycle RMS value of the fundamental frequency component. $X_{Hrms}(h)$ is the h half cycle RMS value of the high-frequency harmonic signal x_H, which contains only the components with frequency ≥ 300 Hz.

$$X_{Hrms}(h) = \frac{1}{\sqrt{2}} \sqrt{\frac{1}{S} \sum_{i=(h-1)S+1}^{hS} x_H(i)^2} \tag{13}$$

F7 This novel feature, mean of the detected half cycle h and its consecutive half cycle of the input signal, $x(i)$ helps in detection of transient, notch, and spike.

$$F7 = \left| \frac{1}{2S} \sum_{i=(h-1)S+1}^{i=(h+1)S} x(i) \right| \tag{14}$$

F8 The discrimination of voltage interruption, sag and swell from each other is possible only with features reflecting the magnitude of the fundamental frequency component. Hence, the per cycle RMS value for ten cycles of the fundamental frequency component is calculated as

$$F8 = \left[X_{rms}(1), \ldots, X_{rms}(n), \ldots, X_{rms}(10) \right] \tag{15}$$

F9 The last feature, mean of the twenty half cycle *HHD* values reflect the presence of high-frequency harmonic distortion over the complete input signal.

$$F9 = mean(HHD) \tag{16}$$

3.2 Dual FFNN classifier

ANNs are the most suitable classifiers because of its parallel information processing capability. FFNN is one such ANN, in which the information flows strictly in a forward direction from input units to outputs. This approach employs a dual FFNN consisting of two independent networks, FFNN1 and FFNN2 for classification of 18 disturbances. The dual FFNN, shown in Figure 5 has eight output neurons corresponding to each single disturbance with flag either 0 or 1 indicating the presence of the disturbance. A threshold value of 0.5 is chosen to push the output to either one or zero. The combinations of these outputs help in the detection of combined PQ disturbances. FFNN1 having 15 input neurons and four output neurons is trained with the first seven features (*F*1–*F*7) as inputs for classification of the disturbances associated with flicker, transient, notch and spike. FFNN2 needs the last two features *F*8 and *F*9 for classifying voltage interruption, sag, swell, and harmonics. The FFNN2 contains 11 neurons in the input layer and four in the output layer. The selection of network parameters and layers is quite tricky but can be solved by trial and error with basic knowledge on the complexity of the problem, the number of inputs and outputs. The classification of combined PQ is a non-linearly separable problem, and the size of the hidden layer is usually greater than the size of the input layer. Therefore, considering one hidden layer with 15 neurons at the start, experimentation has been carried out by monitoring the performance difference in terms of accuracy and computational time. Two hidden layers with log-sigmoid and tan-sigmoid activation functions, respectively, and 30 hidden neurons are found to be optimal for the dual feed-forward network. The training is performed using the Levenberg-Marquardt algorithm (Rodriguez et al., 2014). The list of PQ disturbances considered in this paper is presented in Table 1. The disturbances listed in Table

One is associated with the distribution system voltage. The current signals are also distorted, but usually due to some undesirable frequency components. Therefore, only transient and harmonics/interharmonics disturbance are considered for classification in the case of current signals.

Figure 5 Dual FFNN

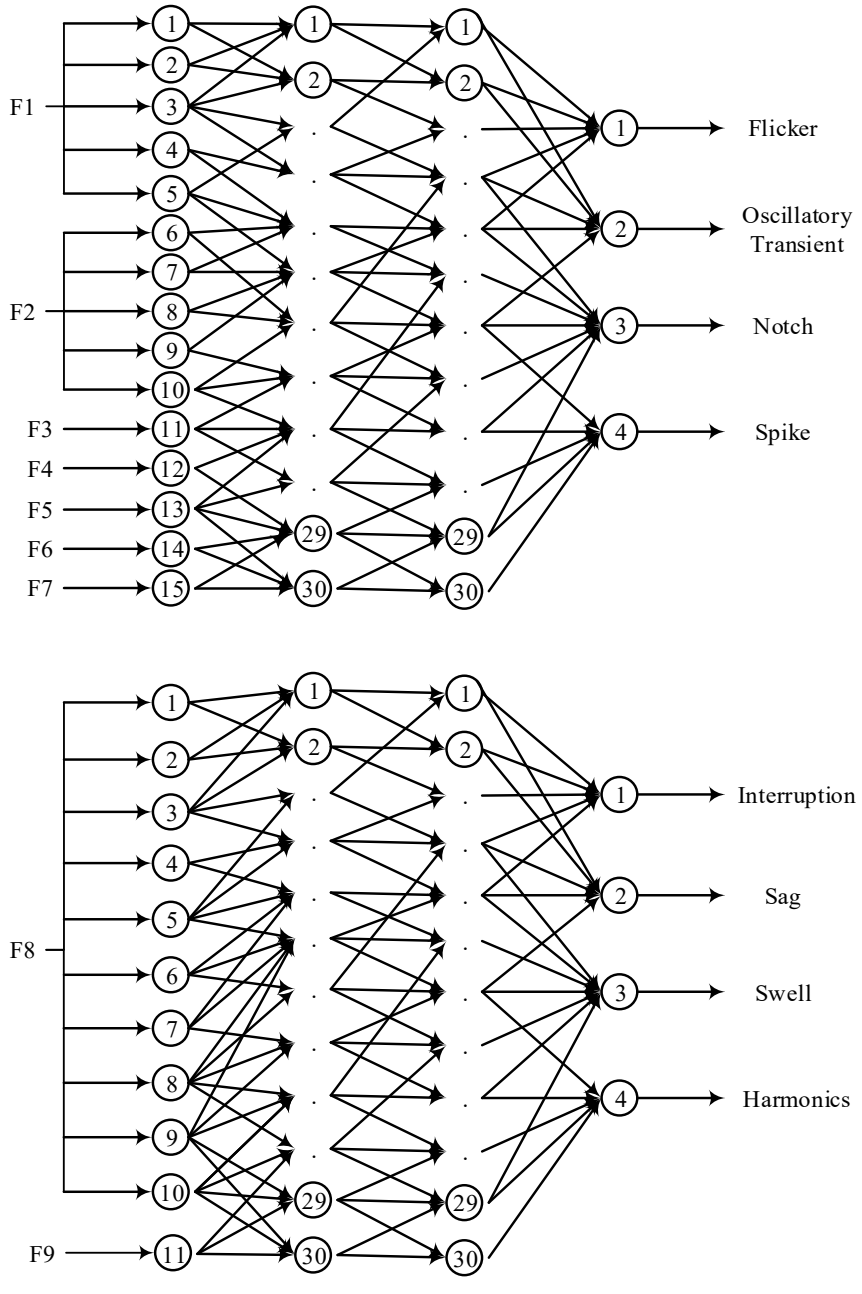

Table 1 Classification accuracy results of the proposed approach for several disturbances

Class labels	*PQ disturbance*	*Classification accuracy (%) with different SNRs*			
		25 dB	*35 dB*	*45 dB*	*Noiseless*
C1	Normal	96	97	99	99
C2	Interruption	97	99	100	100
C3	Sag	96	97	97	97
C4	Swell	98	100	100	100
C5	Harmonics	95	95	96	99
C6	Flicker	95	96	97	97
C7	Oscillatory transient	100	100	100	100
C8	Notch	100	100	100	100
C9	Spike	94	94	95	96
C10	Interruption + transient	96	96	97	98
C11	Sag + harmonics	95	97	97	99
C12	Sag + flicker	96	96	96	98
C13	Sag + osc. transient	92	93	93	95
C14	Swell + harmonics	93	95	96	98
C15	Swell + flicker	100	100	100	100
C16	Swell + osc. transient	93	94	94	95
C17	Harmonics + flicker	100	100	100	100
C18	Harmonics + transient	96	96	96	97
C19	Flicker + transient	93	94	96	96
Average accuracy	Single disturbances	96.87	97.625	98.12	98.62
	Combined disturbances	95.4	96.1	96.5	97.6
	Overall	96.05	96.78	97.31	98.1

4 Results and discussions

4.1 Detection of simulated disturbances

In this paper, eight single and ten two-combination disturbances are considered for analysis along with a pure sinusoidal signal. A complete set of 7,600 patterns with 400 patterns of each class are generated by varying the parameters (Lee and Shen, 2011) and duration of an event. To verify the robustness of the proposed approach, the synthetic signals are contaminated with the additive white Gaussian noise of SNR varying from 25 dB to 55 dB. Further, different phase angles are also considered with a fundamental frequency variation of ±0.5 Hz. The 50 Hz fundamental frequency signals of 200 ms are generated at a sampling rate of 10 kHz, yielding 2,000 samples per window. The dual FFNN classifier is initially trained with 75% of the total patterns, i.e., 300 of each disturbance and the remaining for evaluating the dual FFNN. The initial weights are chosen randomly and the accuracies reported are an average of 15 multiple runs.

Table 1 lists the classification accuracy of all disturbances individually at different noise levels. In the case of noiseless signals, the overall average recognition accuracy is 98.1% with a minimum accuracy of 95% noticed for few combined disturbances containing transient. The sag with transient is misclassified as a sag signal, which is a consequence of very low-intensity transient present in the signal. The same reason holds for the swell with transient and flicker with a transient. In noisy case, few voltage interruption signals are being treated as sag signals due to the drop in voltage to about 0.1 pu for a very short duration (<0.5 cycle). It is also noticed that some flicker signals are misclassified as normal sinusoidal signal owing to the fact that the flicker frequency is just 5 Hz with less magnitude. Similarly, the sag with harmonics and swell with harmonics are recognised as single disturbances if the THD of those signals is below 4%. Even in noisy environment with different SNRs, the single disturbances are recognised accurately except spike. In case of both notch and spike, the disturbance half cycle will be mostly the first cycle and there is a chance of confusion among notch and spikes. The overall accuracy at 25 dB SNR is found to be around 96% with a minimum accuracy of 92% obtained for sag with transient class.

To further exploit the performance of the proposed approach, experiments are done by extending the number of classes to 25 with the inclusion of harmonic with interharmonics class and five other three combination disturbances. The three combination disturbances considered in this work are sag + harmonic + flicker, sag + harmonic + transient, swell + harmonic + flicker, swell+ harmonic + transient and flicker + harmonic + transient. The classification accuracies for the three cases are reported in Table 2, where the network is particularly trained and tested for the mentioned classes. It is observed that the misclassification of combined disturbances to either of the single disturbance class having near similar characteristics increases with an increase in combinations. For instance, sag + harmonic + transient signals are being detected as sag + harmonic and flicker + harmonic + transient signal as a harmonic + transient signal. Thus, the classifier trained for detection of all 25 classes shows reduced performance than that trained for 19 classes and eight classes. Although the classification accuracy of three combination disturbances dropped, the overall accuracy obtained for both noiseless and noisy conditions are still considerable.

Table 2 Classification accuracy results obtained for various disturbances

Dual FFNN	*Classification accuracy (%)*							
	Nine classes	*19 classes*			*25 classes*			
	Average	*Single*	*Two combined*	*Average*	*Single*	*Two combined*	*Three combined*	*Average*
Noisy	97.65	96.87	95.4	96.05	94.25	90.81	86.6	91.32
Noiseless	99.2	98.62	97.6	98.1	97.375	95.09	91.4	95.24

Table 3 Performance comparison for noisy and noiseless disturbances

	ST and PNN (Mishra et al., 2008)		*ST and dynamics (He et al., 2013)*		*ADALINE and FFNN (Rodriguez et al., 2014)*		*SSD and DT (Manikandan et al., 2015)*		*FDST and DT (Biswal and Dash, 2013)*		*Proposed approach*	
Classes	*Noise*	*NL*	*Noise*	*NL*	*Noise*	*NL*	*Noise*	*NL*	*Noise*	*NL*	*Noise*	*NL*
C1	99	100	96	100	90	100	100	100	-	-	96	99
C2	99	99	85	98	100	100	98	100	100	98.67	97	100
C3	98	95	95	100	98	100	100	100	100	96.67	96	97
C4	92	91	97	100	99	100	100	100	-	-	98	100
C5	95	96	97	100	90	98	100	100	100	99.33	95	99
C6	82	98	91	98	87	94	100	100	-	-	95	97
C7	86	100	97	100	86	98	100	100	99.33	100	100	100
C8	99	99	94	99	85	97	98.67	100	100	100	100	100
C9	99	98	94	99	90	97	100	100	-	-	94	96
C10	-	-	-	-	-	-	100	100	-	-	96	98
C11	98	98	95	99	89	98	83.33	84.67	74	96	95	99
C12	-	-	-	-	85	93	97.33	97.33	100	100	96	98
C13	-	-	-	-	86	97	100	100	95.33	100	92	95
C14	84	98	97	99	88	97	82.67	86	-	-	93	98
C15	-	-	-	-	83	93	98	98	100	100	100	100
C16	-	-	-	-	87	98	100	100	98	96	93	95
C17	-	-	-	-	85	94	90	91.33	100	100	100	100
C18	-	-	-	-	86	96	-	-	-	-	96	97
C19	-	-	-	-	83	93	100	100	-	-	93	96
Accuracy	93.19	97.19	94.36	99.19	88.64	96.64	96.94	97.49	96.96	98.78	96.05	98.1

Table 4 Features extracted and results of real disturbance signals

Features	*Harmonic signal (CFL)*	*Voltage harmonic signal (Tiwari et al., 2016)*	*Voltage sag (IEEE 1159.2)*	*Normal voltage signal*	*Transient signal*
H	1	3	10	1	7
Inputs to FFNN1					
F1	43	9	127	32	87
	44	16	0	44	21
	41	39	0	52	15
	0	0	0	0	5
	0	0	0	0	0
F2	10.636	3.58	1.2527	13.148	4.3683
	3.640	8.976	3.8053	23.534	8.9827
	12.536	12.067	4.6849	24.009	14.340
	24.661	12.111	4.8101	16.381	3.5638
	22.993	10.428	2.3653	4.4471	30.362
F3	0.9667	1.100	0.2051	0.9985	1.1759
F4	0.0021	0.067	0.0266	0.003	0.2112
F5	0.9507	1.031	0.2133	0.9773	0.5268
F6	0.1839	0.087	0.0817	0	1.2305
F7	0.002	0.0275	0.0108	0.0003	0.067
Inputs to FFNN2					
F8	0.9452	1.0330	0.9802	0.9917	0.4985
	0.9387	1.0320	0.9695	1.0003	0.4215
	0.9369	1.0341	0.9819	0.9951	0.4657
	0.9384	1.0344	0.9634	0.9984	0.6690
	0.9411	1.0339	0.4895	0.9976	0.8842
	0.9291	1.0334	0.1930	0.9976	0.9570
	0.9424	1.0340	0.5189	0.9975	1.0419
	0.9372	1.0348	0.9309	0.9963	1.0202
	0.9395	1.0339	0.9452	0.9995	1.0499
	0.9385	1.0304	0.9449	0.9989	0.9673
F9	0.1893	0.0877	0.045	0	0.4542
Class detected	C5	C5	C3	C1	C18

Further, the performance of the proposed approach concerning classification accuracy is compared with the other reported techniques, listed in Table 3. It can be observed that the overall classification accuracy of all the methods is almost same for noiseless signals and is sufficient for classification of PQ disturbances. The ANN-based approach (Rodriguez et al., 2014) proposed for classification of 96 disturbances reports a minimum accuracy of 90% for all combinations. However, in a noisy environment, the accuracy of most of the disturbances drops by about 10%. Same is the case with the reported ST-based approaches (Mishra et al., 2008; He et al., 2013; Biswal and Dash, 2013). The sparse signal decomposition (SSD) with a hierarchical DT (Manikandan et al., 2015) performs better in the detection of single disturbances but fails for few combined disturbances.

This comparative study reveals that the proposed approach is appropriate for classification of single and the most frequent combined disturbances.

Figure 6 Real disturbance signals and the detected half cycle (see online version for colours)

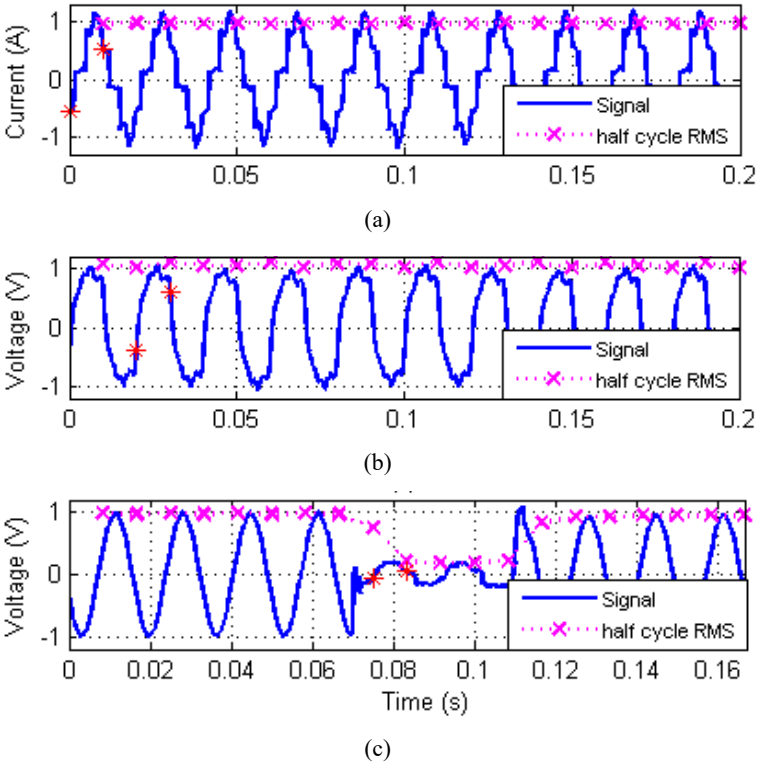

4.2 Detection of real disturbances

Lastly, the proposed approach has been tested on five real disturbance signals acquired in the laboratory using an OROS-34 data acquisition card (DAQ). The signals obtained are first normalised and then the features are obtained, which are listed in Table 4. Considering the fact that the non-linear loads are the major contributors of harmonics, current drawn by CFL lamps, shown in Figure 6(a), is acquired at a sampling rate of 6.4 kHz. The current signal is stationary as can also be seen from the feature $F4$ and thereby the first half cycle, marked in Figure 6(a), is identified for further analysis. The signal decomposition reveals that the signal has only odd harmonics with a considerable high-frequency harmonic distortion of $F6 = 0.1839$. Besides, the features $F6$ and $F9$ are very near and the values of $F4$ and $F7$ are quite low, clearly indicating the disturbance as harmonics but not transient. Similarly, the classifier is tested on another 6.4 kHz harmonic voltage signal, shown in Figure 6(b), which is obtained from distribution system of an academic institution (Tiwari and Jain, 2016). The amplitude of the voltage signal is slightly varying and therefore the third half cycle is detected as the disturbance half cycle. The observations made above remains same for this voltage signal as well and henceforth, the disturbance is detected as a harmonic class ($C5$). In addition, the network

model is validated on a 15.36 kHz sampled 60 Hz voltage sag signal, shown in Figure 6(c), provided by IEEE 1159.2 ('a' phase voltage of wave 7). The $h = 7$ indicates the correct identification of half cycle, which contain disturbance. The features, $F3 = 0.2051$, $F5 = 0.2133$ and $F8$ clearly specifies a drop in the voltage magnitude. Although the harmonic distortion of the half cycle $F6$ is noticed to be considerable due to the relatively less fundamental amplitude, the mean ($F9$) is below 5%. Then, a normal voltage signal sampled at 12.8 kHz is acquired at a single phase distribution panel board of the institute and the results are presented in Table 4. Furthermore, to verify the performance of the classifier on a real transient signal, a switching transient is created by turning on a PC while mobile and laptop are already charging. The obtained features $F4$, $F6$, $F7$, and $F9$ reflect the presence of transient in one half cycle and harmonics throughout the signal. In conclusion, it can be observed that the proposed approach is able to recognise the real-life disturbances correctly, proving its practicality.

4.3 Discussions

The duration of time window length is a very important choice for the detection and classification of PQ disturbances. An increase in window length would increase the non-stationary nature of the signal along with the computational time. For instance, a signal of 2 s duration may contain two or more disturbances, which in turn increases the complexity of detection. Besides, it delays the estimation as the time needed for acquiring the signal is 2 s. In contrary, a short window of one cycle fails to identify the low-frequency interharmonics below 50 Hz. Also, the proposed approach is based on the FFT for frequency estimation and hence, holds the limitation of fixed time-frequency resolution. The better frequency resolution obtained by increasing the time window helps in accurate estimation of all harmonics an interharmonics but simultaneously degrades the time resolution. The opposite may increase the picket fencing effect.

Another vital feature that plays a crucial role in the online classification of PQ disturbances is the total detection time. The total detection time includes the time for signal decomposition, feature extraction and testing. Since the training of the network is performed offline, the training time is not a major concern for the detection of PQ disturbances. All the computations are performed in MATLAB tool hosted on a PC with 3.1 GHz, Core i5 processor, and 4 GB RAM. The testing time completely depends on the neural network model and a number of input features. The number of features remains the same for an input pattern irrespective of its type, sampling rate, and number of frequencies present in the signal. Consequently, the time required for testing a pattern will be almost the same and is found to be near about 20 ms. The experiments carried out indicate that the computations involved in signal decomposition and feature extraction depends on two factors, the number of frequencies and the number of samples of the discrete signal. An increase in either the sampling frequency or the number of frequencies present in the signal will certainly increase the computation time. For instance, the time taken for signal decomposition and feature extraction of 10 kHz harmonic signal with nine frequencies is found to be around 26.3 ms. While for a transient signal with approximately thirty frequency components, the decomposition and the feature extraction time is at most 70 ms. The overall mean computation time for decomposition, feature extraction and recognising a PQ disturbance present in the signal of 200 ms duration (2000 samples) is found to be 58.9 ms. After successful estimation of frequencies, the filters can be built simultaneously for obtaining the individual frequency components.

Furthermore, the feature extraction and the two FFNNs can also be executed in parallel, which can further reduce the computational time. Therefore, implementation of the proposed approach on digital signal processor or FPGA can make the approach suitable for real-time detection of the most significant PQ disturbances.

5 Conclusions

This paper presents a new approach with EWT-based adaptive filtering and a dual FFNN for classification of single and combined disturbances. The advantage of the computational efficiency of the FFT and adaptiveness of the filter design makes the adaptive filtering technique suitable for decomposing the distortion signal quickly and accurately. Features extracted from this adaptive filtering technique are significant and non-complex. Further, the use of ANN having one output neuron dedicated for a single disturbance helps in recognising the combined disturbances and also improves the robustness to noise. Finally, the experimentations carried out with the simulated as well as a few real power signals clearly reveal the speed, accuracy and practical applicability of the proposed approach.

References

Abdoos, A.A., Mianaei, P.K. and Ghadikolaei, M.R. (2016) 'Combined VMD-SVM based feature selection method for classification of power quality events', *Appl. Soft Comput.*, Vol. 38, pp.637–646.

Andrade, L.C.M., Oleskovicz, M. and Fernandes, A.S.R. (2016) 'Adaptive threshold based on wavelet transform applied to the segmentation of single and combined power quality disturbances', *Appl. Soft Comput.*, Vol. 38, pp.967–977.

Biswal, M. and Dash, P.K. (2013) 'Detection and characterization of multiple power quality disturbances with a fast S-transform and decision tree based classifier', *Digital Signal Processing*, Vol. 23, No. 4, pp.1071–1083.

Deokar, S.A. and Waghmare, L.M. (2014) 'Integrated dwt-fft approach for detection and classification of power quality disturbances', *Int. J. Electr. Power Energy Syst.*, Vol. 61, pp.594–605.

Dugan, R.C., McGranaghan, M.F. and Beaty, H.W. (2012) *Electrical Power Systems Quality*, McGraw Hill, New York.

Ferreira, D.D., Seixas, J.M. and Cerqueira, A.S. (2015) 'A method based on independent component analysis for single and multiple power quality disturbance classification', *Electric Power Syst. Res.*, Vol. 119, pp.425–431.

Gallo, D., Langella, R. and Testa, A. (2004) 'Desynchronized processing technique for harmonic and interharmonic analysis', *IEEE Trans. Power Del.*, Vol. 19, No. 3, pp.993–1001.

Gilles, J. (2013) 'Empirical wavelet transform', *IEEE Trans. Signal Process.*, Vol. 61, No. 16, pp.3999–4010.

Gilles, J., Tran, G. and Osher, S. (2014) '2d empirical transforms. Wavelets, ridgelets, and curvelets revisited', *SIAM J. Imaging Sci.*, Vol. 7, No. 1, pp.157–186.

He, S., Li, K. and Zhang, M. (2013) 'A real-time power quality disturbances classification using hybrid method based on s-transform and dynamics', *IEEE Trans. Instrum. Meas.*, Vol. 62, No. 9, pp.2465–2475.

Hu, G., Zhu, F. and Ren, Z. (2008) 'Power quality disturbance identification using wavelet packet energy entropy and weighted support vector machines', *Expert Systems with Applications*, Vol. 35, No. 2, pp.143–149.

IEC (2002) *IEC Standard 61000-4-7. General Guide on Harmonics and Interharmonics Measurements, for Power Supply Systems and Equipment Connected Thereto*.

IEEE (2009) *IEEE Recommended Practice for Monitoring Electric Power Quality*, IEEE Std., pp.1159–2009.

IEEE 1159.2 (2001) *Working Group, Test Waveforms* [online] http://grouper.ieee.org/groups/1159/2/testwave.html (accessed May 2015).

Kanirajan, P. and Kumar, V.S. (2015) 'Power quality disturbance detection and classification using wavelet and RBFNN', *Appl. Soft Comput.*, Vol. 35, pp.470–481.

Krishna, B.V. and Baskaran, K. (2013) 'Parallel computing for efficient time-frequency feature extraction of power quality disturbances', *IET Signal Processing*, Vol. 7, No. 4, pp.312–326.

Lee, C.Y. and Shen, Y.X. (2011) 'Optimal feature selection for power-quality disturbances classification', *IEEE Trans. Power Del.*, Vol. 26, No. 4, pp.2342–2351.

Lieberman, D.G., Troncoso, R.J.R., Rios, R.A.O., Perez, A.G. and Yepez, E.C. (2011) 'Techniques and methodologies for power quality analysis and disturbances classification in power systems: a review', *IET Gen. Transm. Distrib.*, Vol. 5, No. 4, pp.519–529.

Liu, Z., Cui, Y. and Li, W. (2015) 'A classification method for complex power quality disturbances using EEMD and rank wavelet SVM', *IEEE Trans. Smart Grid*, Vol. 6, No. 4, pp.1678–1685.

Manikandan, M.S., Samantaray, S. and Kamwa, I. (2015) 'Detection and classification of power quality disturbances using sparse signal decomposition on hybrid dictionaries', *IEEE Trans. Instrum. Meas.*, Vol. 64, No. 1, pp.27–38.

Milanovic, J.V., Meyer, J. et al. (2014) 'International industry practice on power-quality monitoring', *IEEE Trans. Power Del.*, Vol. 29, No. 2, pp.934–941.

Mishra, S., Bhende, C.N. and Panigrahi, B.K. (2008) 'Detection and classification of power quality disturbances using S-transform and probabilistic neural network', *IEEE Trans. Power Del.*, Vol. 23, No. 1, pp.280–287.

Panigrahi, B.K. and Pandi, V.R. (2009) 'Optimal feature selection for classification of power quality disturbances using wavelet packet-based fuzzy k-nearest neighbour algorithm', *IET Gen. Transm. Distrib.*, Vol. 3, No. 3, pp.296–306.

Rodriguez, M.V., Troncoso, R.D.J.R., Rios, R.A.O. and Perez A.G. (2014) 'Detection and classification of single and combined power quality disturbances using neural networks', *IEEE Trans. Ind. Electron.*, Vol. 61, No. 5, pp.2473–2482.

Saini, M.K. and Kapoor R. (2012) 'Classification of power quality events – a review', *Int. J Electr. Power Energy Syst.*, Vol. 43, No. 1, pp.11–19.

Santoso, S., Powers, E.J., Grady, W.M. and Parsons, A.C. (2000) 'Power quality disturbance waveform recognition using wavelet-based neural classifier-part 2: application', *IEEE Trans. Power Del.*, Vol. 15, No. 1, pp.229–235.

Thirumala, K., Maganuru, S.P., Jain, T. and Umarikar, A.C. (2016) 'Tunable-Q wavelet transform and dual multiclass SVM for online automatic detection of power quality disturbances', *IEEE Trans. Smart Grid*, in press.

Thirumala, K., Umarikar, A.C. and Jain, T. (2015) 'Estimation of single-phase and three-phase power-quality indices using empirical wavelet transform', *IEEE Trans. Power Del.*, Vol. 30, No. 1, pp.445–454.

Tiwari, V.K. and Jain, S.K. (2016) 'Hardware implementation of polyphase-decomposition-based wavelet filters for power system harmonics estimation', *IEEE Trans. Inst. Meas.*, Vol. 65, No. 7, pp.1585–1595.

Zeng, B., Zhou, Y., Teng, Z. and Li, G. (2013) 'A novel approach for harmonic parameters estimation under nonstationary situations', *Int. Jour. of Elect. Power and Energy Systems*, Vol. 44, No. 1, pp.930–937.

Zhang, M., Li, K. and Hu, Y. (2011) 'A real time classification method for power quality disturbances', *Electric Power Syst. Res.*, Vol. 81, No. 1, pp.660–666.